Published in final edited form as:

Ophthalmol Retina. 2020 November ; 4(11): 1059–1068. doi:10.1016/j.oret.2020.05.001.

Hyperreflective foci and specks are associated with delayed rod-mediated dark adaptation in non-neovascular age-related macular degeneration

Benjamin S. Echols, MD[1], **Mark E. Clark, BS**[1], **Thomas A. Swain, MPH**[1,2], **Ling Chen, MD PhD**[1], **Deepayan Kar, MS**[3], **Yuhua Zhang, PhD**[4], **Kenneth R. Sloan, PhD**[1], **Gerald McGwin Jr, PhD**[1,2], **Ramya Singireddy, MD**[1], **Christian Mays, MD**[1], **David Kilpatrick, MD**[5], **Jason N. Crosson, MD**[1,5,*], **Cynthia Owsley, PhD**[1,*], **Christine A. Curcio, PhD**[1]

[1]Department of Ophthalmology and Visual Sciences, School of Medicine, University of Alabama at Birmingham, Birmingham AL USA;

[2]Department of Epidemiology, School of Public Health, University of Alabama at Birmingham, Birmingham AL USA;

[3]Vision Science Training Program, University of Alabama at Birmingham, Birmingham AL USA;

[4]Doheny Eye Institute, Department of Ophthalmology, University of California at Los Angeles, Los Angeles CA USA;

[5]Retina Consultants of Alabama, Birmingham AL USA

Abstract

PURPOSE: Hyperreflective foci (HRF) are optical coherence tomography (OCT) biomarkers for progression of non-neovascular age-related macular degeneration (AMD) attributed to anteriorly migrated retinal pigment epithelial (RPE) cells. We examined associations between rod- and cone-mediated vision and HRF plus smaller hyperreflective specks (HRS); we sought a histologic candidate for HRS.

DESIGN: cross-sectional study; histologic survey

PARTICIPANTS: Patients with normal maculas (n=34), early AMD (N=26), and intermediate AMD (N=41)

METHODS: AMD severity was determined via the 9-step Age-Related Eye Disease Study scale. In OCT scans HRF and HRS were manually counted. Vision tests probed cones (best corrected visual acuity (VA), contrast sensitivity), mixed cones and rods (low luminance VA, low luminance deficit, mesopic light sensitivity), or rods (scotopic light sensitivity, rod-mediated dark adaptation (RMDA)). An online AMD histopathology resource was reviewed.

Correspondence: Christine A. Curcio, PhD; Department of Ophthalmology and Visual Sciences; EyeSight Foundation of Alabama Vision Research Laboratories; 1670 University Boulevard Room 360; University of Alabama at Birmingham School of Medicine; Birmingham AL 35294-0099; christinecurcio@uabmc.edu.

*equal contributions

Financial conflict of interest:

Dr. Curcio receives research support from Heidelberg Engineering and Genentech/ Hoffman LaRoche and is a stockholder of MacRegen. Dr. Owsley is a patent holder on the AdaptDx. Dr. Sloan is a stockholder of MacRegen.

MAIN OUTCOME MEASURES: Vision in eyes assessed for HRF and HRS; candidate histology for HRS.

RESULTS: In 101 eyes of 101 patients, HRF and HRS were identified in 25 and 95 eyes, respectively, with good intra- and inter-rater reliability. HRF were present but sparse in normal eyes, infrequent in early AMD eyes, and frequent but highly variable among intermediate AMD eyes (number per eye, 0.1±0.2, 0.2±0.5, 1.9 ± 3.4; normal, early, intermediate, respectively). HRS outnumbered HRF in all groups (4.5 ± 3.2; 6.3±5.8; 19.4 ± 22.4). Delayed RMDA was strongly associated with more HRF and HRS (both $p<0.0001$). HRF were also associated with worse low luminance VA ($p=0.0117$). HRS were associated with worse contrast sensitivity ($p=0.0278$), low luminance VA ($p=0.0010$), low luminance deficit ($p=0.0031$), and mesopic ($p=0.0018$) and scotopic sensitivity ($p<0.0001$). By histology, cone lipofuscin was found in inner segments, and the outer nuclear and Henle fiber layers of 25% of normal aged eyes.

CONCLUSIONS: HRF and HRS are markers of cellular activity associated with visual dysfunction, especially delayed RMDA, an AMD risk indicator assessing efficiency of retinoid re-supply. HRS may represent lipofuscin granules translocating inwardly within cone photoreceptors. Visible and quantifiable on SD-OCT, HRF and HRS may serve as structural endpoints in clinical trials targeting AMD stages earlier than atrophy expansion. These results should be confirmed in a larger sample.

Précis

In patients with age-related macular degeneration (intermediate, n=41; early, n=26) and in normal controls (n=34), the number of hyperreflective foci and specks were associated with delayed rod-mediated dark adaptation, a functional test of the capacity for retinoid transfer and replenishment.

Keywords

Optical coherence tomography; hyperreflective foci; retinal pigment epithelium; rod-mediated dark adaptation; cone-mediated vision; age-related macular degeneration; fundus grading; lipofuscin; subretinal drusenoid deposits

Introduction

Age-related macular degeneration (AMD) is the fourth largest cause of vision loss globally. [1] Neovascular complications are managed with anti-vascular endothelial growth factor therapy, [2] and some patients with intermediate AMD benefit from dietary antioxidant supplementation. [3] Recent clinical trials of new drugs for AMD failed to meet primary endpoints of slowing the expansion of geographic atrophy (GA), [4, 5] the only anatomic endpoint currently approved by regulatory agencies. GA involves intense photoreceptor depletion and reactive gliosis that may be irreversible. [6] Thus, therapies and appropriate endpoints for earlier AMD stages are needed. Because the subcellular-level detail routinely available in optical coherence tomography (OCT) has impacted all aspects of retinal disease diagnosis and management, an international consensus group recommended OCT as a base modality for AMD clinical trials.[7] Accordingly, OCT indicators of progression and progression risk are of interest.

Hyperreflective foci (HRF) in AMD are well-circumscribed lesions within the neurosensory retina with a reflectivity similar to the retinal pigment epithelium (RPE). [8] HRF were linked to migrating RPE in proliferative vitreoretinopathy [9] and in AMD, correlated to hyperpigmentation on color fundus photography (CFP). [10] In longitudinal studies HRF at baseline confer risk for progression to advanced AMD (odds ratio, OR, and 95% confidence interval), OR = 11 (2.5–50.0), 4.7 (2.4–9.8), 6.5 (2.8–14.7), at last follow-up, two years, and five years, respectively [10–12]). Sadda and coworkers proposed a four-biomarker composite risk score [8] that includes presence of HRF, subretinal drusenoid deposits, and heterogeneous internal druse reflectivity (calcific nodules), [13] plus drusen volume. Among these biomarkers, the risk for GA onset in eyes fellow to neovascular AMD in a prospective trial imaging dataset was largest for HRF (OR, 5.21 (3.29–8.26) at 24 months).[14] In high-resolution histology paired with longitudinal OCT imaging [15] HRF in non-neovascular AMD were directly correlated to nucleated and fully pigmented RPE that either singly or in groups left the RPE layer following a local disturbance and migrated into the retina. [16] Hypoxia may drive anterior migration of RPE. [15] As reviewed, [15] oxygenation is theoretically reduced atop drusen, and once in the retina, RPE contact retinal capillaries and express vascular endothelial growth factor. In neovascular AMD, HRF also include lipid-filled cells of possible immune origin. [17]

Rod-mediated dark adaptometry (RMDA) is a psychophysical technique that assesses integrity of retinoid re-supply to rod photoreceptors in the macula, from plasma through choriocapillaris endothelium, Bruch's membrane (BrM), and RPE. For the recovery of rod sensitivity after a bright light flash, re-supply is rate-limiting. [18] RMDA is a suitable outcome measure for aging and AMD, because it assesses the same pathology [19] that may also drive individual RPE cells to migrate anteriorly. Unlike rods, cones have a second delivery route via Müller glia, which are additionally sustained by the retinal circulation.[20] Thus at early stages of AMD, cone-mediated vision will be less impaired than rod-mediated vision. Indeed, delayed RMDA at baseline in eyes considered normal confers risk for AMD onset three years later; [21] deficits in cone-mediated vision do not. [22] In intermediate AMD, RMDA tracks progression at two [23] and four years' [24] follow-up.

Stabilizing or reducing the number of HRF has potential as an outcome for trials targeting early and intermediate AMD. Validating an anatomic biomarker includes demonstrating its relationship to visual function. Vision is important to patients and to regulatory agencies. Herein we assess in an initial study the impact of HRF on cone- and rod-mediated visual function in the macula. We also explore small and numerous features, called hyperreflective specks (HRS), that appear in the Henle fiber and outer nuclear layers (HFL, ONL; Figure 1) of normal aged as well as AMD eyes. We demonstrate that functionally relevant cellular activity is observable by high-quality OCT. The relative merits of HRF and HRS as outcome measures for AMD trials are discussed.

Methods

The study followed the tenets of the Declaration of Helsinki and was approved by the Institutional Review Board at the University of Alabama at Birmingham (UAB; protocol

170324006). Study participants provided written informed consent after the nature and purpose of the study were described.

Participants were recruited from the comprehensive eye care and retina clinics in the Callahan Eye Hospital at UAB. One eye of each participant was required to meet criteria for normal macular health, early AMD, or intermediate AMD. Three-field digital stereo-CFP (Carl Zeiss Meditec 450+, Dublin, CA) were evaluated by an experienced grader (MEC) masked to other study variables (intra-observer agreement κ =0.88, inter-observer agreement κ =0.75). Eyes receiving a step of 1 in the AREDS 9-step classification system (Table 8 of [25]) were defined as normal. Exclusion criteria included central or non-central GA, neovascularization, previous diagnoses of glaucoma, retina and optic nerve conditions, corneal disease, brain injury, diabetes, or neurological or psychiatric conditions as revealed by the medical record or self-report. Suspects for non-symptomatic type 1 neovascularization were excluded by a consultant experienced with OCT angiography and the double-layer sign in structural OCT. [26] Demographic characteristics (age, sex, race/ethnicity) were obtained through participant interview.

We acquired spectral-domain OCT volumes of all maculas (Spectralis HRA + OCT, Heidelberg Engineering, Heidelberg, Germany; λ = 870 nm; scan depth, 1.9 mm; axial resolution, 3.5 μm per pixel in tissue; lateral resolution, 14 μm per pixel in tissue). B-scans (n=73) were horizontally oriented and centered over the fovea in a 20° × 15° (5.7 × 4.2 mm) area. Automatic Real-Time averaging was 8–18, and quality (signal-to-noise) was 20–47 dB. A retina fellow (DK) under supervision of a fellowship-trained retina specialist (JNC), masked to all participant characteristics except OCT, evaluated OCT volumes. Each B-scan for each eye was assessed for specific pathologies commonly encountered in a retina practice, which were then annotated in the database. Specific items on the review checklist are summarized in our previous publication in which we evaluated normal eyes, as determined by CFP, for pathology on OCT. [27] OCT graders looked for each disorder in every OCT volume.

OCT analysis

Reflectivity of HRF is similar to or more intense than the RPE-BrM band. While reviewing B-scans for HRF, we identified reflective features that were smaller, less reflective, and more uniform in size than HRF and called these HRS. In preliminary studies, we checked HRF and HRS reflectivity at high magnification, enforcing a 3-pixel minimum for HRF, as recommended. [8] HRS were too small to measure reliably. If a candidate lesion was large and dim, then it was scored as HRF, because it is known that inwardly migrating cells could change shape and lose granules [6] and thus reflectivity. If a group of candidate HRF/ HRS was not internally separated by hyporeflectivity when viewed at Auto magnification, then the lesion was scored as one HRF. Included with HRF were reflective features that were detached internally from an intact RPE layer but still external to the ELM. These were believed to represent Sloughed RPE of histology. [28] Figure 1 shows how HRF and HRS were identified in AMD and normal eyes. HRF and HRS could be found overlying uniform RPE (**B,D**) as well as over drusen (**A,C**) in AMD eyes. HRF and HRS were also found over uniform RPE in normal eyes (Figure 1E,F).

The reviewer (MEC) began by reviewing all B-scans at Auto magnification (113%) to identify major features. Then, again at this magnification, the reviewer started at the left edge of each scan and checked the overall disposition of the EZ, attending especially to RPE elevations. Candidate lesions were reviewed at higher magnification (up to 200%) and on one scan on either side of the index scan, using the orientation line to maintain position. The identity of reflective features could be verified by context on the index scan and presence/absence on an adjacent scan.

Subretinal drusenoid deposits (SDD) are independently associated with delayed RMDA.[29, 30] To determine if associations of visual performance with HRF and HRS was affected by SDD, we determined SDD presence using SD-OCT-anchored multimodal imaging, assisted by reference to a stack of near-infrared and autofluorescence images co-registered to the SD-OCT volume (author KRS; ImageJ v1.52; NIH, Bethesda, MD, USA) [31] SDD presence was defined as at least 5 definite drusenoid lesions in the subretinal space, using published criteria for stages 1–3 [32] (Supplementary Figure 1). B-scans were reviewed by author DK at 100% magnification for EZ non-uniformity and inspected at 125% magnification for SDD. If the area of suspected SDD extended outside the SD-OCT volume, SDD had to be visible as either solid or annular hyporeflective lesions in a distinct punctate pattern on near-infrared reflectance imaging [32] or multiple hypoautofluorescent lesions in a pattern on fundus autofluorescence [33]

Intra and inter-rater reliability was determined independently for HRF, HRS, and SDD. Prior to reviewing all eyes, 20 eyes were randomly selected for assessment of the OCT B-scans by primary and secondary reviewers using the same methods. The primary reviewer then completed the assessment on the same 20 eyes again. Intra and inter-rater reliability for the number of HRF and HRS per eye were calculated as the intraclass correlation coefficient using the Shrout-Fleiss reliability method (fixed set). Intra and inter-reliability for SDD presence were assessed using the kappa statistic. Once the intra and inter-rater reliability were established, the primary reviewer completed the OCT assessment of all eyes.

Visual function testing

Rod-mediated dark adaptation (RMDA) was measured psychophysically (AdaptDx, MacuLogix, Harrisburg, PA) [21, 34]in one eye after dilation, i.e., the eye with better best-corrected visual acuity, because of time constraints in the study visit. The procedure began with a photo-bleach exposure to a flash (0.25 ms duration, 58,000 scotopic cd/m^2 s intensity; equivalent ~83% bleach) while the participant focused on the fixation light. The photo-bleach flash was a 6° square centered at 5° on the inferior vertical meridian (i.e. superior to the fovea on the retina). This was also the position of the test target. Threshold measurement for a 2° diameter circular target of 500 nm wavelength (green) light began 15 seconds after bleach offset, with participants pressing a button when a flashing target first became visible. Log thresholds were expressed as sensitivity in decibel (dB) units as a function of time after bleach offset. Dark adaptation speed is defined by the rod intercept time (RIT), the duration in minutes required for sensitivity to recover to a criterion value of 5.0×10^{-3} scotopic cd/m^2, in the latter half of the second component of RMDA.[18, 34]

The eye tested for RMDA underwent additional vision tests, as follows. Best-corrected visual acuity was assessed via the Electronic Visual Acuity tester (EVA; JAEB Center, Tampa FL) under photopic conditions (expressed as logarithm of the minimum angle of resolution, logMAR). Low luminance visual acuity was also assessed using the EVA with participants viewing letters through a 2.0 log unit neutral density filter to reduce luminance to 1 cd/m^2. Low luminance deficit was defined by the increase in logMAR under mesopic conditions as compared to photopic conditions. Contrast sensitivity was estimated by the Pelli-Robson chart (Precision Vision, La Salle, IL) under photopic conditions and scored by the letter-by-letter method. Mesopic and scotopic sensitivity was measured using the MP1-S microperimeter (Nidek Technologies, Padova, Italy), modified to increase the dynamic range of target light intensity to 30 dB. Using a Goldmann III target (0.43° degrees diameter), sensitivity was measured at the fovea and 4 targets on each side of the fovea on the horizontal and vertical meridians, out to 12° eccentricity (17 total targets). Sensitivity was expressed as average sensitivity among all 17 test targets. Not all participants had microperimetry testing, because the instrument was not available.

Statistical analysis

Data on sample demographics, AMD severity, visual function tests, retinal pathologies, HRF, and HRS were reported at the eye level. AMD severity was categorized as normal (AREDS 1), early (AREDS 2–4), and intermediate (AREDS 5–8). Linear regression models were used to associate the continuous visual function tests (dependent variables) and AMD disease severity category (independent variable), adjusted for age. Counts of HRF and HRS per eye were modeled as dependent variables with relation to AMD disease severity category, adjusted for age, using Poisson regression. The association of the number of foci and specks with visual function tests were assessed using Pearson partial correlations, accounting for age. In addition to age, SDD were added to models to examine how associations were attenuated. The level of significance was 0.05. All analyses were completed using SAS version 9.4 (SAS Institute, Cary, NC).

Histology study

Because HRS were found in normal as well as AMD eyes, we sought candidate reflectors by reviewing histology of normal aged eyes. The Project MACULA online resource displays high-resolution epoxy resin histology of 55 normal aged eyes (31 female, 24 males, mean age 79.7±9.8 years), as described. [35] Eyes are represented by 0.8-μm-thick sections, one through the rod-free fovea and another 2 mm superior to the fovea, on the inner slope of the perifoveal ring of high rod density. Our initial hypothesis based on observations in advanced AMD[6] was that HRS represent RPE organelles dispersed from degenerating RPE in its layer, taken up by Müller glia, and translocated within glia to the HFL. Guided by our published images of intracellular [16] and extracellular [6] RPE organelles in normal and AMD eyes, sections were reviewed online by author BSE to identify features in the bacillary layer, ONL, and HFL with reflective potential. Of the identified candidates, many were intracellular inclusions in cone photoreceptors, i.e., a known age-related lipofuscin unique to cones. [36, 37] All candidates were verified, imaged, and enumerated on the original glass slides by author LC using a 60X oil objective (numerical aperture, 1.42; Olympus VSI 120, CellSens; Olympus, Center Valley PA).

Results

Table 1 shows person-level characteristics of the cohort, which was comprised of 101 individuals, 56.4% women, and 98% white of European descent. Of the tested eyes, 34 (33.7%) were normal, 26 (25.7%) were early AMD, and 41 (40.6%) were intermediate AMD, according to the CFP-based 9-step AREDS scale. As we previously showed, [27] a small proportion of eyes considered normal by CFP exhibit pathology when examined by OCT (**Supplementary Table 2**). Two eyes met OCT criteria for complete RPE and outer retinal atrophy (cRORA) [38] but were retained in the analysis, because they met the original CFP-based grading criteria. Nine eyes exhibited various other pathologies that were considered non-contributory. Inter-rater reliability for count of HRF and HRS per eye was 0.9697 and 0.9548, respectively. Intra-rater reliability was 0.8424 and 0.9566 for count of HRF and HRS at the eye level.

Table 2 shows the results of visual function tests and the distribution of HRF and HRS, stratified by AMD presence and severity. Except for BCVA, all visual functions, whether mediated by cones, cones and rods together, or rods only, worsened with increasing AMD severity. Table 2 also shows that both HRF and HRS were found more frequently in eyes at higher levels of AMD severity. HRF were present but averaged near 0 in normal eyes; they were infrequent in early AMD eyes, and more frequent although highly variable in intermediate AMD eyes. Interestingly, HRS were regularly found in normal eyes (Figure 1E), much more so than HRF (4.5 ± 3.2 vs 0.1 ± 0.2). They were also found often in intermediate AMD eyes, much more than HRF (19.4 ± 22.4 vs 1.9 ± 3.4), although both were variable at all AMD severities. In normal eyes, HRS were numerous (23 to >100) in 19% of the eyes. The majority of eyes (81%) had fewer than 20 HRS per eye. The number of HRF and HRS per eye were highly correlated (r=0.60, p=<0.0001). It should be emphasized that HRF and HRS counts underestimate the true total, because it was not possible to sample the 60-μm-wide-space between scans in the OCT volumes.

Table 3 shows the age-adjusted association for HRF and HRS with visual function. HRF counts were strongly associated with RMDA (Pearson partial correlation, r=0.38; p<0.0001) as well as low luminance acuity, but more modestly (r=0.25, p=0.0117). HRS counts were significantly associated with many aspects of cone- and rod-mediated function including contrast sensitivity, low luminance acuity, low luminance deficit, and mesopic sensitivity, but not with visual acuity. HRS's strongest relationships with visual functions were those with major or exclusive rod contribution, i.e., RMDA, scotopic sensitivity, and mesopic sensitivity (r=0.57, −0.46, and −0.36, respectively). The strongest association across all measures for both HRF and HRS was RMDA. In this cohort 58% of eyes were found to have SDD, which have been previously associated with delayed RMDA. [29, 30] Intra- and inter-grader reliability (both 0.6939) were considered moderate for SDD. Associations between visual function and HRF and HRS were similar when adjusting for SDD. For example, the association between RIT and HRF decreased from r=0.38 (P<0.0001) to r=0.34 (p=0.0005); between RIT and HRS, associations decreased from r=0.57 (p<0.0001) to r=0.52 (p<0.0001) when accounting for age and SDD.

Figure 2 shows examples of cone lipofuscin in normal aged eyes, offered as a possible histologic correlate of HRS. These deeply stained ovoid structures 1–2 μm in diameter may be single or clustered. They are classically found in the myoid portion of cone inner segments (IS, Figure 2B). They were also observed crossing the ELM (Figure 2C), within photoreceptor cell bodies in the ONL (Figure 2D), and within fibers of the HFL (Figure 2E). Figure 2E shows in one section the similar morphology of organelles in the IS, near the ELM, and the HFL. These inclusions were confirmed in 16 sections of 14 eyes (25.5% of total eyes reviewed): IS (13 sections), ONL (10 sections), HFL (5 sections), and OPL (1 section).

Discussion

In a sample of intermediate AMD, early AMD, and normal eyes, we find that HRF are associated with delayed RMDA and less strongly to cone-mediated or mixed cone- and rod-mediation. We also documented that small reflective features called HRS are present in normal as well as AMD eyes. Relative to HRF, HRS are more numerous, and are more strongly associated with delayed RMDA. Here we consider the neurophysiologic underpinnings and implications of our test outcomes, HRF and HRS identity, the potential of HRF as a functionally validated endpoint for clinical trials in early disease, and the potential of HRF to inform care of older patients with and without AMD.

HRF and HRS are most strongly associated with delayed RMDA, as compared to other aspects of cone and combined cone-rod function tests, whose associations with HRF and HRS are either weaker or non-existent. HRF confer increased risk for AMD progression. [10–12, 14] We also know that delayed RMDA increases risk for incident AMD, [21] whereas cone dysfunction does not. RMDA also becomes more accentuated as AMD progresses. [23] By finding a HRF and RMDA association, we have functionally validated a structural characteristic known to increase risk for advanced AMD. HRF have been proposed as a potentially useful structural endpoint for studies on preventing intermediate AMD's transition to advanced disease. [39] Preserving the structural integrity of the macula is key in claiming treatment success in AMD trials, yet patients gauge treatment success by the quality of their vision. By selecting structural endpoints in AMD trials that have been functionally validated, both benchmarks are more likely to be met -- arresting anatomical disease progression and preventing further vision loss. Further, delays in RMDA are associated with difficulty and emotional distress experienced by older adults when performing visual activities under dim illumination and at night (driving, reading, detecting objects, ambulatory mobility). [40] Problems with low luminance tasks are predictive of progression. [41]

Our functional data lend support for quantifying HRF as outcome measures for trials targeting processes early in AMD progression, i.e., before possibly irreversible damage. Recently Schaal and Rosenfeld [42] elaborated a rationale for an anatomic endpoint composed of growth of drusen volume, formation of GA, and formation of neovascularization. They further proposed that modulating an intermediate AMD feature, such as drusen volume, already associated with high risk of progression would be an attractive outcome. HRF are known to also confer high risk for progression, even more than drusen in some populations;

strong evidence supports that they are anteriorly migrating RPE. A measure of RPE health atop drusen, such as stability of HRF with concomitant lack of neovascularization or atrophy, thus has merit as a readout of treatment efficacy. This approach is valuable for therapies expected to de-toxify drusen, [43] i.e., by removing or neutralizing one component without necessarily reducing overall drusen volume. This scenario requires careful selection of trial patients to include those with pre-existing HRF to indicate an appropriate level of overall disease activity.

To our knowledge, our study of HRF is the first to include normal eyes, thus allowing us assess limits to feature visibility in OCT. Consensus OCT nomenclature recognizes a wide hyporeflective band that includes both HFL and ONL, [44] the separate contributions of which are visualizable by varying the entry angle of light. [45] Against the background of this optically pristine tissue, imaged under high signal-to-noise conditions, it may be possible to detect features smaller than the instrumental resolution limits. Our previous histology studies identified in the HFL-ONL of advanced AMD eyes groups of RPE, individual RPE, clusters of RPE organelles, and individual melanosomes. [6, 16, 28] We previously confirmed that cells are detectable by OCT but whether grouped or isolated organelles are detectable is currently unknown. Indeed, we determined that the relationships with different visual functions hold even if HRF and HRS are combined, on the grounds that they both indicate cellular activity.

We hypothesize from the current data that lipofuscin translocating from cone IS is reflective and visible. The similar proportions of older eyes with cone lipofuscin visible by histology (25%) and those with abundant HRS by OCT (19%) suggests that this notion is plausible. Inclusion bodies in cone photoreceptor IS of adult human retina were first described thirty years ago. [36, 37] Cone lipofuscin granules are solitary, refractile, [46] autofluorescent, [37] and distinct from other organelles in cones [47] and from RPE lipofuscin. [48] In outer retinal tubulation, cone lipofuscin n enlarges, acquires different staining properties, and translocates inwardly. [49] We found that HRS were positively associated with RIT, i.e., more were visible as rod sensitivity recovery slowed. Why would cone lipofuscin translocate if RMDA is slowed? Although rods are reliably impaired earlier and more severely than cones in aging and AMD, cones are not unaffected. [22, 50, 51] Our histology findings, representing a snapshot in time, may signify that translocation of cone lipofuscin from IS to HFL inner fibers is a marker of cellular response to stress. Some degree of cone stress is expected, because cones depend on the failing choriocapillaris-Bruch's membrane-RPE complex even while being sustained by Müller glia. HRS may be more useful as biomarkers than HRF, because they are numerous. On the other hand, reliable detection of HRS in B-scans may require a higher-than-typical signal-to-noise ratio (quality metric).

In addition to application in clinical trials, HRF are readily identifiable and potentially quantifiable in the clinic setting, offering the potential for risk stratification of older patients with and without AMD. In this initial study we used 73 B-scans, more than is typical in clinical usage (e.g., 19 scans). It might be possible to detect the same associations using fewer scans. We cannot address this question in this cohort, because the associations with RIT were driven by a small number of participants. To support using fewer scans, a study with more eyes overall, more eyes with HRF and HRS, and comprehensive measures of total HRF and HRS is needed; our ongoing prospective study will address these points. If

applied to B-scans of sufficient quality to capture fine structural detail like HRS, machine-learning methods may prove useful for screening and diagnosis. Further, efficient detection and quantification of HRF via *en face* OCT has recently been demonstrated. [39] Another structural OCT measure of RPE health, hypertransmission stripes attributed to mild RPE degeneration, [52] also has merit as a trial outcome measure.

Study strengths are multimodal vision function testing, high-quality OCT scans, reliable manual counts by a trained observer, and novel observations of HRS in normal older eyes with a plausible histologic correlate. Limitations addressable in future studies include small cohort size, the small number of HRF, lack of other anatomic outcomes, and AMD staging by CFP, which is standardized but limited in sensitivity. In conclusion, HRF and HRS are markers of cellular activity associated with visual dysfunction, especially delayed RMDA, an AMD risk indicator that assesses efficiency of retinoid re-supply. HRS may represent lipofuscin granules translocating inwardly within cone photoreceptors. If confirmed, our data support the concept that subcellular detail is available to clinical decision making and theories of outer retinal disease via signal averaged, eye-tracked OCT. Because HRF and HRS are visible and quantifiable on high-quality OCT, they may serve as structural endpoints in clinical trials targeting AMD stages earlier than atrophy expansion.

Supplementary Material

Refer to Web version on PubMed Central for supplementary material.

Acknowledgements

We thank Maximillian Pfau MD for consultation on non-exudative neovascular AMD.

Financial support:

NIH grants R01AG04212, R01EY029595; R01EY027948; R01EY024378; Center for Clinical and Translational Science TL1TR001418 training grant ; EyeSight Foundation of Alabama; Dorsett Davis Discovery Fund; Alfreda J. Schueler Trust; Research to Prevent Blindness Inc; Heidelberg Engineering; Macula Foundation.

References

1. Flaxman SR, Bourne RRA, Resnikoff S, et al. Global causes of blindness and distance vision impairment 1990–2020: a systematic review and meta-analysis. Lancet Glob Health 2017;5(12):e1221–e34. [PubMed: 29032195]
2. Maguire MG, Martin DF, Ying GS, et al. Five-year outcomes with anti-vascular endothelial growth factor treatment of neovascular age-related macular degeneration: the Comparison of Age-Related Macular Degeneration Treatments Trials. Ophthalmology 2016;123(8):1751–61. [PubMed: 27156698]
3. Age-Related Eye Disease Study 2 Research Group. Lutein + zeaxanthin and omega-3 fatty acids for age-related macular degeneration: the Age-Related Eye Disease Study 2 (AREDS2) randomized clinical trial. JAMA 2013;309(19):2005–15. [PubMed: 23644932]
4. Rosenfeld PJ, Dugel PU, Holz FG, et al. Emixustat hydrochloride for geographic atrophy secondary to age-related macular degeneration: a randomized clinical trial. Ophthalmology 2018;125(10):1556–67. [PubMed: 29716784]
5. Holz FG, Sadda SR, Busbee B, et al. Efficacy and safety of lampalizumab for geographic atrophy due to age-related macular degeneration. Chroma and Spectri phase 3 randomized clinical trials. JAMA Ophthalmol 2018;136(6):666–77. [PubMed: 29801123]

6. Li M, Huisingh C, Messinger JD, et al. Histology of geographic atrophy secondary to age-related macular degeneration: a multilayer approach. Retina 2018;38(10):1937–53. [PubMed: 29746415]
7. Holz FG, Sadda S, Staurenghi G, et al. Imaging protocols for clinical studies in age-related macular degeneration – recommendations from Classification of Atrophy (CAM) Consensus Meeting. Ophthalmology 2017;124(4):464–78. [PubMed: 28109563]
8. Lei J, Balasubramanian S, Abdelfattah NS, et al. Proposal of a simple optical coherence tomography-based scoring system for progression of age related macular degeneration. Graefes Arch Clin Exp Ophthalmol 2017;255(8):1551–8. [PubMed: 28534244]
9. Zacks DN, Johnson MW. Transretinal pigment migration: an optical coherence tomographic study. Arch Ophthalmol 2004;122(3):406–8. [PubMed: 15006864]
10. Christenbury JG, Folgar FA, O'Connell RV, et al. Progression of intermediate age-related macular degeneration with proliferation and inner retinal migration of hyperreflective foci. Ophthalmology 2013;120(5):1038–45. [PubMed: 23352193]
11. Ouyang Y, Heussen FM, Hariri A, et al. Optical coherence tomography-based observation of the natural history of drusenoid lesion in eyes with dry age-related macular degeneration. Ophthalmology 2013;120(12):2656–65. [PubMed: 23830761]
12. Sleiman K, Veerappan M, Winter KP, et al. Optical coherence tomography predictors of risk for progression to non-neovascular atrophic age-related macular degeneration. Ophthalmology 2017;124(12):1764–77. [PubMed: 28847641]
13. Tan AC, Pilgrim M, Fearn S, et al. Calcified nodules in retinal drusen are associated with disease progression with age-related macular degeneration. Sci Transl Med 2018;10:466–77.
14. Nassisi M, Lei J, Abdelfattah NS, et al. OCT risk factors for development of late age-related macular degeneration in the fellow eyes of patients enrolled in the HARBOR study. Ophthalmology 2019.
15. Curcio CA, Zanzottera EC, Ach T, et al. Activated retinal pigment epithelium, an optical coherence tomography biomarker for progression in age-related macular degeneration. Invest Ophthalmol Vis Sci 2017;58(6):BIO211–BIO26. [PubMed: 28785769]
16. Balaratnasingam C, Messinger JD, Sloan KR, et al. Histologic and optical coherence tomographic correlations in drusenoid pigment epithelium detachment in age-related macular degeneration. Ophthalmology 2017;124(1):644–56. [PubMed: 28153442]
17. Li M, Dolz-Marco R, Messinger JD, et al. Clinicopathologic correlation of anti-vascular endothelial growth factor-treated type 3 neovascularization in age-related macular degeneration. Ophthalmology 2018;125(2):276–87. [PubMed: 28964579]
18. Lamb TD, Pugh EN Jr. Dark adaptation and the retinoid cycle of vision. Prog Retin Eye Res 2004;23(3):307–80. [PubMed: 15177205]
19. Curcio CA, Owsley C. Rod-mediated dark adaptation as a suitable outcome for early and intermediate age-related macular degeneration. Ophthalmology 2019;126(6):866–7. [PubMed: 31122362]
20. Saari JC. Vitamin A and Vision. Subcell Biochem 2016;81:231–59. [PubMed: 27830507]
21. Owsley C, McGwin G Jr., Clark ME, et al. Delayed rod-mediated dark adaptation is a functional biomarker for incident early age-related macular degeneration. Ophthalmology 2016;123(2):344–51. [PubMed: 26522707]
22. Owsley C, Clark ME, Huisingh CE, et al. Visual function in older eyes in normal macular health: association with incident early age-related macular degeneration 3 years later. Invest Ophthalmol Vis Sci 2016;57(4):1782–9. [PubMed: 27074381]
23. Owsley C, Clark M, McGwin G Jr. Natural history of rod-mediated dark adaptation over two years in intermediate age-related macular degeneration. Transl Vis Sci Technol 2017;6(3):15.
24. Chen KG, Alvarez JA, Yazdanie M, et al. Longitudinal study of dark adaptation as a functional outcome measure for age-related macular degeneration. Ophthalmology 2019;126(6):856–65. [PubMed: 30278196]
25. Age-Related Eye Disease Study Research Group. The Age-Related Eye Disease Study severity scale for age-related macular degeneration: AREDS Report No. 17. Arch Ophthalmol 2005;123(11):1484–98. [PubMed: 16286610]

26. Shi Y, Motulsky EH, Goldhardt R, et al. Predictive value of the OCT double-layer sign for identifying subclinical neovascularization in age-related macular degeneration. Ophthalmology Retina 2019;3(3):211–9. [PubMed: 31014697]
27. Crosson JN, Swain TA, Clark ME, et al. Retinal pathologic features on OCT among eyes of older adults judged healthy by color fundus photography. Ophthalmology Retina 2019;3(8):670–80. [PubMed: 31103641]
28. Zanzottera EC, Messinger JD, Ach T, et al. The Project MACULA retinal pigment epithelium grading system for histology and optical coherence tomography in age-related macular degeneration. Invest Ophthalmol Vis Sci 2015;56(5):3253–68. [PubMed: 25813989]
29. Flamendorf J, Agron E, Wong WT, et al. Impairments in dark adaptation are associated with age-related macular degeneration severity and reticular pseudodrusen. Ophthalmology 2015;122(10):2053–62. [PubMed: 26253372]
30. Lains I, Miller JB, Mukai R, et al. Health conditions linked to age-related macular degeneration associated with dark adaptation. Retina 2017.
31. Schindelin J, Arganda-Carreras I, Frise E, et al. Fiji: an open-source platform for biological-image analysis. Nat Methods 2012;9(7):676–82. [PubMed: 22743772]
32. Zweifel SA, Imamura Y, Spaide TC, et al. Prevalence and significance of subretinal drusenoid deposits (reticular pseudodrusen) in age-related macular degeneration. Ophthalmology 2010;117(9):1775–81. [PubMed: 20472293]
33. Spaide RF, Ooto S, Curcio CA. Subretinal drusenoid deposits a.k.a. pseudodrusen. Surv Ophthalmol 2018;63(6):782–815. [PubMed: 29859199]
34. Mullins RF, McGwin G Jr, Searcey KB, et al. ARMS2 A69S polymorphism associates with delayed rod-mediated dark adaptation in eyes at risk for incident age-related macular degeneration. Ophthalmology 2019;126(4):591–600. [PubMed: 30389424]
35. Dolz-Marco R, Glover JP, Litts KM, et al. Choroidal and sub-retinal pigment epithelium caverns: multimodal imaging and correspondence with Friedman lipid globules. Ophthalmology 2018;125(8):1287–301. [PubMed: 29625839]
36. Tucker GS. Refractile bodies in the inner segments of cones in the aging human retina. Invest Ophthalm Vis Sci 1986;27(5):708–15.
37. Iwasaki M, Inomata H. Lipofuscin granules in human photoreceptor cells. Invest Ophthalmol Vis Sci 1988;29(5):671–9. [PubMed: 3366562]
38. Sadda SR, Guymer R, Holz FG, et al. Consensus definition for atrophy associated with age-related macular degeneration on optical coherence tomography: CAM Report 3. Ophthalmology 2018;125(4):537–48. [PubMed: 29103793]
39. Nassisi M, Fan W, Shi Y, et al. Quantity of intraretinal hyperreflective foci in patients with intermediate age-related macular degeneration correlates with 1-year progression. Invest Ophthalmol Vis Sci 2018;59(8):3431–9. [PubMed: 30025092]
40. Owsley C, McGwin G Jr., Scilley K, Kallies K. Development of a questionnaire to assess vision problems under low luminance in age-related maculopathy. Invest Ophthalmol Vis Sci 2006;47(2):528–35. [PubMed: 16431946]
41. Ying GS, Maguire MG, Liu C, Antoszyk AN. Night vision symptoms and progression of age-related macular degeneration in the complications of Age-related Macular Degeneration Prevention Trial. Ophthalmology 2008;115(11):1876–82. [PubMed: 18672295]
42. Schaal KB, Rosenfeld PJ, Gregori G, et al. Anatomic clinical trial endpoints for nonexudative age-related macular degeneration. Ophthalmology 2016;123(5):1060–79. [PubMed: 26952592]
43. Rudolf M, Curcio CA, Schlötzer-Schrehardt U, et al. Apolipoprotein A-I mimetic peptide L-4F removes Bruch's membrane lipids in aged non-human primates. Invest Ophthalmol Vis Sci 2019;60(2):461–72. [PubMed: 30707219]
44. Staurenghi G, Sadda S, Chakravarthy U, Spaide RF. Proposed lexicon for anatomic landmarks in normal posterior segment spectral-domain optical coherence tomography: The IN*OCT Consensus. Ophthalmology 2014;121(8):1572–8. [PubMed: 24755005]
45. Lujan B, Roorda A, Knighton RW, Carroll J. Revealing Henle's fiber layer using spectral domain optical coherence tomography. Invest Ophthalmol Vis Sci 2011;52:1486–92. [PubMed: 21071737]

46. Curcio CA, Millican CL, Allen KA, Kalina RE. Aging of the human photoreceptor mosaic: evidence for selective vulnerability of rods in central retina. Invest Ophthalmol Vis Sci 1993;34(12):3278–96. [PubMed: 8225863]

47. Nag TC, Wadhwa S, Chaudhury S. The occurrence of cone inclusions in the ageing human retina and their possible effect upon vision: an electron microscope study. Brain Res Bull 2006;71(1–3):224–32. [PubMed: 17113950]

48. Feeney L Lipofuscin and melanin of human retinal pigment epithelium. Fluorescence, enzyme cytochemical and ultrastructural studies. Invest Ophthalmol Vis Sci 1978;17(7):583–600. [PubMed: 669890]

49. Litts KM, Messinger JD, Zhang Y, et al. Inner segment remodeling and mitochondrial translocation in degenerating cones of age-related macular degeneration, including outer retinal tubulation. Invest Ophthalmol Vis Sci 2015;56(4):2243–53. [PubMed: 25758815]

50. Owsley C, Jackson GR, Cideciyan AV, et al. Psychophysical evidence for rod vulnerability in age-related macular degeneration. Invest Ophthalmol Vis Sci 2000;41(1):267–73. [PubMed: 10634630]

51. Owsley C, McGwin G Jr., Jackson GR, et al. Cone- and rod-mediated dark adaptation impairment in age-related maculopathy. Ophthalmology 2007;114(9):1728–35. [PubMed: 17822978]

52. Xu X, Liu X, Wang X, et al. Retinal pigment epithelium degeneration associated with subretinal drusenoid deposits in age-related macular degeneration. Am J Ophthalmol 2017;175(3):87–98. [PubMed: 27986424]

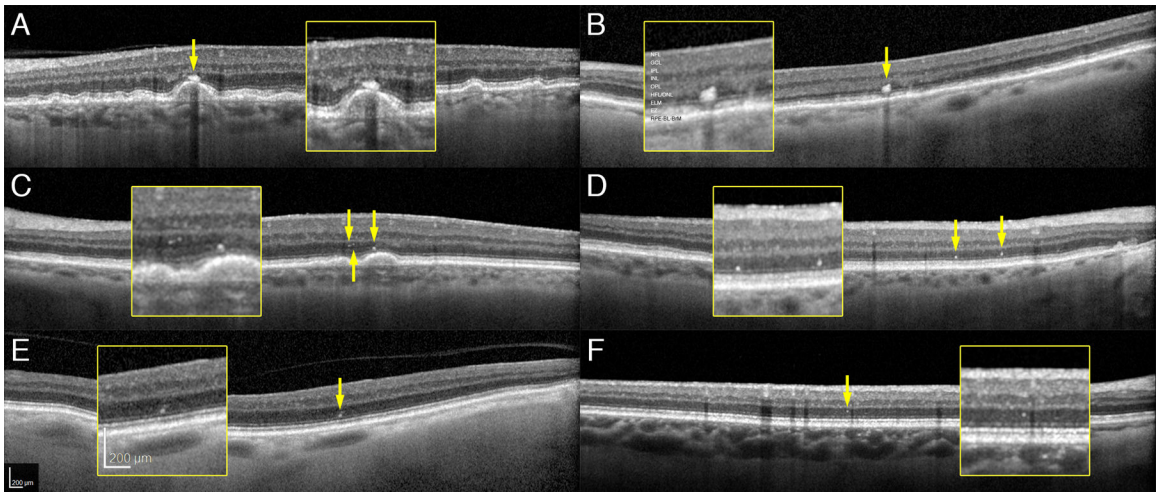

Figure 1: Hyperreflective foci and specks in age-related macular degeneration and aging

Spectral domain optical coherence tomography B-scans of representative cases. NFL, nerve fiber layer, GCL, ganglion cell layer; IPL, inner plexiform layer; OPL, outer plexiform layer; HFL/ONL, Henle fiber layer/ outer nuclear layer; ELM, external limiting membrane; EZ, ellipsoid zone; RPE-BL-BrM, retinal pigment epithelium – basal lamina – Bruch membrane. **A.** Foci overlying drusen (81 years, AREDS 7). **B.** Foci overlying flat RPE (95 years, AREDS 7). **C.** Specks over drusen (87 years, AREDS 7). **D.** Specks overlying flat RPE (82 years old, AREDS 6). **E.** Foci in a normal aged eye (82 years, AREDS 1). **F.** Speck in a normal aged eye (67 years, AREDS 1).

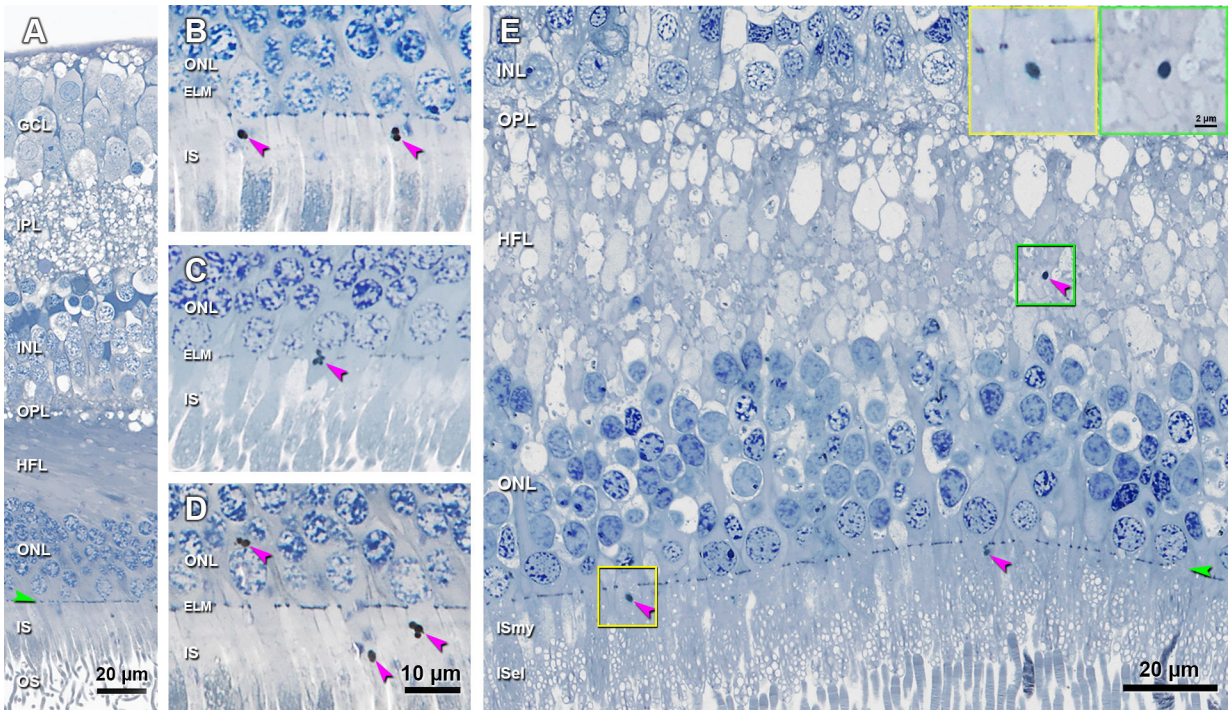

Figure 2. Lipofuscin granules in cone photoreceptors, a candidate for hyperreflective specks.

A. Histology shows normal retinal layers. **B.** Lipofuscin granules are observed in the ISmy of two cone photoreceptors. **C.** A cluster of lipofuscin granules are crossing the ELM in a cone photoreceptor. **D.** Lipofuscin granules are observed inside the cell body of one cone in ONL, and also be found in the ISmy of two other cones. Histology in A-D from a 92-year-old man. **E.** Lipofuscin granule is observed in the HFL (green frame and also green inset), which looks similar to the one in the ISmy of a cone (yellow frame and also yellow inset). These data are consistent with inward translocation of lipofuscin granules within individual cones. A 70-year-old man. GCL, ganglion cell layer; IPL, inner plexiform layer; INL, inner nuclear layer; OPL, outer plexiform layer; HFL, Henle fiber layer; ONL, outer nuclear layer; IS, inner segment; OS, outer segment; ISmy, inner segment myoid; ISel, inner segment ellipsoid. Purple arrowheads, lipofuscin granules; Green arrowheads, ELM. Scale bar in D applies to B-D. Scale bar in the green inset also applies to the yellow inset.

Table 1.

Demographic characteristics and age-related macular degeneration (AMD) severity of 101 participants (eyes = 101).

Mean age	75.4 ± 6.7
Age group, years	
60–69	18 (17.8)
70–79	59 (58.4)
80–89	20 (19.8)
90–95	4 (4.0)
Gender	
Male	44 (43.7)
Female	57 (56.4)
Race	
White, non-Hispanic	99 (98.0)
African American	1 (1.0)
Asian or Pacific Islander	1 (1.0)
AMD severity	
Normal	34 (33.7)
Early	26 (25.7)
Intermediate	41 (40.6)

Mean ± standard deviation or N (%). Percentages might not sum to 100% due to rounding.

Table 2.

Visual function and number of foci and specks per eye in the eye that underwent dark adaptation testing summarized for all participants and stratified by AMD disease severity.

	All Participants	AMD Disease Severity			
	(N = 101)[3]	Normal (N = 34)	Early (N = 26)	Intermediate (N = 41)	p-value
Visual function					
Cone mediated tests					
Best-corrected visual acuity (logMAR)	0.06 ± 0.17	0.04 ± 0.15	0.02 ± 0.14	0.10 ± 0.16	0.0531[1]
Contrast sensitivity (log sensitivity)	1.54 ± 0.13	1.56 ± 0.10	1.60 ± 0.12	1.48 ± 0.14	0.0003[1]
Cone and rod mediated tests					
Low luminance acuity (logMAR)	0.3 ± 0.2	0.2 ± 0.2	0.3 ± 0.2	0.4 ± 0.2	<0.0001[1]
Low luminance deficit	0.3 ± 0.1	0.2 ± 0.1	0.3 ± 0.2	0.3 ± 0.2	0.0003[1]
Mesopic light sensitivity (dB)	22.3 ± 4.2	23.2 ± 4.0	23.8 ± 3.2	20.5 ± 4.5	0.0052[1]
Rod mediated tests					
Scotopic light sensitivity (dB)	15.2 ± 4.0	16.3 ± 2.9	16.7 ± 2.9	13.1 ± 4.8	0.0003[1]
Rod-mediated dark adaptation (RIT)	20.0 ± 13.6	15.6 ±10.2	14.6 ± 6.4	26.9 ± 16.4	<0.0001[1]
Foci and specks					
Number of foci per eye	0.8 ± 2.3	0.1 ± 0.2	0.2 ± 0.5	1.9 ± 3.4	<0.0001[2]
Number of specks per eye	11.0 ± 16.1	4.5 ± 3.2	6.3 ± 5.8	19.4 ± 22.4	<0.0001[2]

Mean ± standard deviation

AMD = age-related macular degeneration; RIT = rod intercept time; MAR = minimum angle of resolution

[1]From linear regression for continuous visual function, dependent variable, with AMD disease severity, independent variable, age adjusted

[2]From Poisson regression for count variable, dependent, by AMD severity, independent variable, age adjusted

[3]75 participants completed mesopic and scotopic light sensitivity testing (28 normal, 19 early, and 28 intermediate)

Table 3.

Association of number of foci and specks per eye (n=101)[1] with visual function in the eye that underwent dark adaptation testing.[2]

	Number of foci per eye		Number of specks per eye	
	Correlation coefficient	**p-value**	**Correlation coefficient**	**p-value**
Best-corrected visual acuity (logMAR)	0.15	0.1264	0.16	0.1082
Contrast sensitivity (log sensitivity)	−0.14	0.1786	−0.22	0.0278
Low luminance acuity (logMAR)	0.25	0.0117	0.33	0.0010
Low luminance deficit	0.20	0.0513	0.29	0.0031
Mesopic light sensitivity	−0.15	0.1957	−0.36	0.0018
Scotopic light sensitivity	−0.16	0.1695	−0.46	<0.0001
Rod-mediated dark adaptation (RIT)	0.38	<0.0001	0.57	<0.0001

RIT=rod intercept time; MAR=minimum angle of resolution

[1]101 participants (eyes) underwent all visual function testing except mesopic and scotopic light sensitivity, which 75 participants (eyes) completed

[2]Association from Pearson partial correlation coefficient, adjusted for age. For positive correlations, increases in the value associated with the visual function test indicate worse function. For negative correlations, decreases in the value associated with the visual function test indicate worse function. While not all associations are significant, all correlations show poorer function with increases in the number of foci and specks.